International Journal of Applied Mathematics
Volume 38 No. 7s, 2025
ISSN: 1311-1728 (printed version); ISSN: 1314-8060 (on-line version)

AGRICULTURAL ASSESSMENT USING AERIAL-IMAGERY DATA WITH DEEP CONVOLUTION NETWORK AND PRESCRIPTION MAP ALGORITHM FOR OPTIMIZED SPRAYING PATH

Gouri Pandey , Yuvraj Borad [1], Harsh Sharma[1], Surender Kannaiyan [1]

Visvesvaraya National Institute of Technology,Nagpur,Maharashtra,@India 440010)

*Corresponding author: Gouri Pandey

Other authors: harshgsharma2002@gmail.com, yuviborade28@gmail.com, ksurender@ece.vnit.ac.in

Visvesvaraya National Institute of Technology, Nagpur Maharashtra, 440 010 (India)

E-mail: gouripandey1210@gmail.com

Abstract

This work presents the use of unmanned aerial vehicles (UAVs) within precision agriculture for weed segmentation and variable rate application (VRA) in precision agriculture. Conventional spraying methods often lack precision, leading to environmental and economic concerns. Leveraging deep learning techniques, we propose a solution to tackle these challenges efficiently. This research addresses these issues using drone imagery and deep-learning techniques for site-specific weed management. Our work combines Semantic segmentation of the crop fields and prescription map analysis to model itself as an end-to-end detection system for field surveillance. The Deep Convolutional Networks are employed to predict weed infestation in the field. We employed three diverse datasets, including one collected under Indian conditions, ensuring the robustness and applicability of our approach across different agricultural settings. Using semantic mapping, we calculated prescription maps for specific land patches, determining the spraying required in each area. This data is then utilized to guide a UAV sprayer along an optimized spraying path for the field. By planning an optimized trajectory, the sprayer can efficiently travel the shortest distance while delivering the necessary amount of spray in each region. This study also includes a comparative analysis of three distinct path-planning approaches (1) the lawnmower algorithm, (2) the Priority-based algorithm, and (3) the TSP-based algorithm to determine their suitability for optimizing field coverage and resource management in drone-based missions. Using the RGB-based data the model achieved an overall accuracy of 92.22% whereas with modified data it achieved 95.04%. Experimental results showed that both deep learning models led to high segmentation accuracy. Still, the model trained on the transformed data had accuracy 2.82% higher than the RGB data-based model. Our analysis focused on priority-based and Traveling Salesman Problem (TSP)-based methods, among others. The findings demonstrate that both priority-based and Traveling Salesman Problem (TSP)-based methods show promising results in optimizing field coverage and resource utilization.

Received: August 09, 2025

International Journal of Applied Mathematics
Volume 38 No. 7s, 2025
ISSN: 1311-1728 (printed version); ISSN: 1314-8060 (on-line version)

Keywords: Semantic segmentation, Deep Convolutional Networks, prescription map, semantic mapping, agriculture environment.

1. Introduction

Agriculture contributes to 20.2 percent of the GDP [1]. Several activities based around the agriculture sector, contribute directly or indirectly towards the total yield. One of the most prominent activity is the pesticide application [2]. The spraying application of pesticides requires a deep understanding of the crops, the weed infestation rate, and the local knowledge of the crops which is passed down from generation to generation in farmers. The chemicals to be sprayed are carefully chosen as per need. Precise spraying with sufficient doses can improve crop health. This also helps in environmental sustainability. Spilling or overdosing can lead to various environmental issues to surroundings and health-related issues with associated workers in the task respectively [3, 4]. Effective cost is also one of the important parameters that must be considered when profit is to be taken into account [5].

One of the most prominent problems that the agriculture sector faces is weed infestation. Weeds are unwanted plants in agricultural fields that affect the overall crop health and yield. To tackle such challenges various measures have been adopted such as increasing spraying efficiency using various equipment, use of plant protection products (PPPs) [6]. There also exists some problems like an increase in tolerance value to resist the effects of pesticides in weeds, which can also lead to over-spraying [7].

One of the best-suggested methods is to design an accurately variable spray rate technology(VRT) application system based on the weed infestation rate in the field, resulting in better control, less contamination, and resource-saving. Integration with map-based and sensor-based approaches can improve crop yield. A significant amount of previous research has demonstrated the importance of variable-rate spraying in precision agriculture and other similar applications [8]. One such solution discusses the incorporation of AI solutions for site-specific weed management (SSWM) to reduce herbicides that cause toxicity and contamination in nature which pose a threat to human health, losses in biodiversity, and change the local ecosystem [9-11].

Precise spraying eliminates the need for human interference through automated drone missions [12]. This suggests that an end-to-end system can be formed which can combine the data collection and spraying of the required chemicals. To improve and maximize the system's performance, research is still being conducted on the prescription map generation and weed detection module. The end-to-end system has the potential to significantly enhance precision farming, support sustainable resource management, and promote effective crop production methods [13].

2. Related works

Traditionally, to reduce weed growth farmers use suitable chemicals (weedicides) to mitigate their growth. This ensures that all the nutrition should be focussed on the crops. However as discussed in the section (in the introduction), traditional spraying of weedicide might not be efficient and it can impact negatively on the surrounding environment when done for a long

Volume 38 No. 7s, 2025
ISSN: 1311-1728 (printed version); ISSN: 1314-8060 (on-line version)

time. The spread that arises from spraying techniques is also one of the factors that has to be taken into account [10]. To deal with this, there are some approaches such as Ultra-low Volume sprayers (ULV), UAV-based sprayers, and variable rate sprayers [14] which have gained popularity recently. Also, Modern agriculture is forecasted to be the largest usage for specialized UAVs [12]. This is because it reduces human efforts and crop disturbance. Similarly, Aerial visual recognition has gained increasing attention in the agriculture sector. An autonomous UAV (integrated with different sensors) can fly over a field to produce a map that can be used for further processing. Several vision-based solutions for agricultural domains have been developed such as semantic segmentation for the detection of weed infestation in the fields [15]. This is possible by the public availability of large-scale agriculture vision datasets [16].

With advances in Deep Learning, feature extraction methods can perform much better than conventional image processing-based methods. However, the detection of weeds among growing plants is still a challenging task. Sometimes they can be separated from a line of crops as they grow in between the planted crops. Most of the time, they are occluded by the crops, also, it becomes difficult when they have the same shape and color and it can be hard even for the human eye to distinguish. The time of detection also serves as an important parameter because the plant properties change as they grow. Some common challenges such as changes in lighting conditions, blurry images due to UAV motion, and lossy texture due to lower resolution are always present when working with images. To address these challenges, various methods are used such as the multispectral cameras to get vegetation indices. One such method is the use of the Normalized Difference Vegetation Index (NDVI) which improves the overall visibility of crop fields [17]. It is also motivated by the use of deep convolution networks (DCNN) which can help in distinguishing different features between crops and weeds [18]. Increasing the number of convolution layers in networks can help in solving complex tasks but it also increases the number of parameters and computational cost. Similarly, the use of different scale images for weed detection can be used to extract features at different levels [19]. These hierarchical features then can be used to generate a semantically segmented map of the field.

Remote sensing techniques have also seen significant progress in recent years, enabling the collection of high-resolution data that captures various aspects of complex terrain structures. This allows for detailed descriptions and analyses of both vertical and horizontal distributions of vegetation elements within a forest. UAVs are the basic entity in the field of remote processing UAVs offer several advantages. Their smaller size allows for high-resolution data acquisition at lower flight altitudes [20]. This translates to capturing finer details on the ground compared to sensors on distant platforms. One key advancement is the use of sensors that can detect various parts of the electromagnetic spectrum. These sensors fall into two categories: active and passive. Active sensors, like radar and LiDAR, emit their energy to detect objects and analyze the reflected radiation. Passive sensors, on the other hand, detect natural radiation emitted or reflected by objects, like those in the visible, infrared, and thermal spectrums. Examples include RGB, multispectral, and hyperspectral cameras.

Received: August 09, 2025

International Journal of Applied Mathematics
Volume 38 No. 7s, 2025
ISSN: 1311-1728 (printed version); ISSN: 1314-8060 (on-line version)

3. Data Acquisition

High-resolution image data of the agricultural field is captured using a drone equipped with a camera. We consider two different datasets shown in **Figure 1** to train and validate our model.

- CoFly-WeedDB: It is a custom dataset specifically designed for precision agriculture [22]. It contains 201 RGB images of the cotton field. Its use is limited due to its custom nature and notable class imbalance. It offers aerial images for identifying crops and weeds, supporting machine learning models for crop management and precision agriculture.
- WeedMap Dataset: It is the largest available weed mapping dataset based on spectral mapping [23]. It has a resolution of 1cm/pixel for an image, focuses on weed identification and mapping, providing data for developing algorithms to optimize weed control and reduce herbicide use.

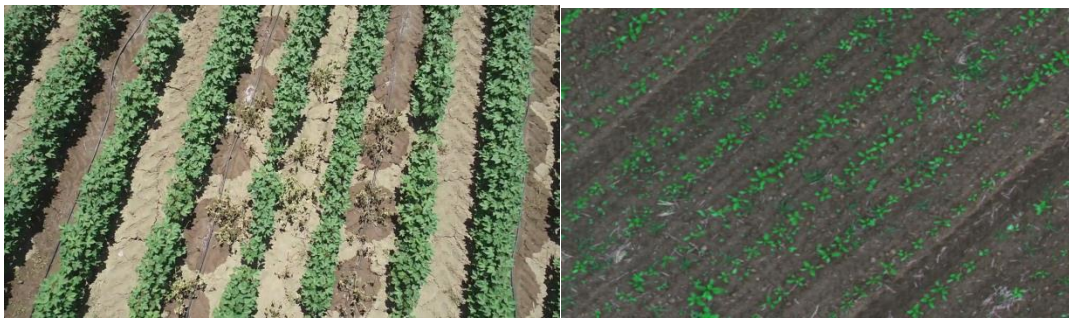

a b

Figure 1 Dataset (a) Co-flyDB (b) WeedMap

It consists of multiple aligned image channels beyond RGB. The additional spectral bands can provide valuable information for weed identification beyond what the human eye can perceive. However, we only use the RGB band images for analysis. There are 8 orthomosaics available, which can aligned image channels beyond RGB. In the problem statement, it is assumed that the drone follows a pre-programmed flight path for data collection.

The data was collected from the Regional Agricultural Research Station, Balasaheb Sawant Konkan Krishi Vidyapith, Raigad, Maharashtra. The dataset consists of 3 crops: 50 images of rice, 419 images of moong shown in **Figure 2**, and 41 images of fodder corn including videos. The images shown are from the field, collected at the Agronomy Farm, Vidhyapith, Raigad. The source of the dataset is mentioned for reference. Over three days, crop images were gathered during morning (9-11 am) and evening (5-7 pm) sessions to account for different lighting conditions. We also ensured data collection under both cloudy and clear weather conditions to provide a comprehensive dataset. This approach allows for an evaluation of the dataset's performance across varying environmental factors. We focused on annotating moong data for Mosiac disease [24] and The rice data for weed infestation identified Phyllanthus niruri, commonly known as gale of the wind or stonebreaker, as the weed species present and overall crop health. For testing purposes, rice and moong bean were selected due to the distinct yet representative characteristics of their leaves.

Received: August 09, 2025

International Journal of Applied Mathematics
Volume 38 No. 7s, 2025
ISSN: 1311-1728 (printed version); ISSN: 1314-8060 (on-line version)

a b

Figure 2 (a) Moong field (b) Moong Dataset Images

We also utilized a DJI Mavic 3 Pro drone to gather aerial images of vegetation and fields. The DJI Mavic 3 Pro features a 20MP Hasselblad 4/3 CMOS sensor with 5.1K resolution at 50fps for high-quality RGB imaging. It includes telephoto lenses and utilizes Hasselblad's Natural Colour Solution for accurate colors. Operating in the 2.4–5.8 GHz bands, it offers stable video transmission up to 15 km but lacks built-in radiometric calibration for multispectral or thermal imaging. **Figure 3** displays a drone-captured image taken from a height of 10 meters of a landscape near a Moong crop field, providing a detailed view that includes treetops and shrubs for a comprehensive analysis of the area.

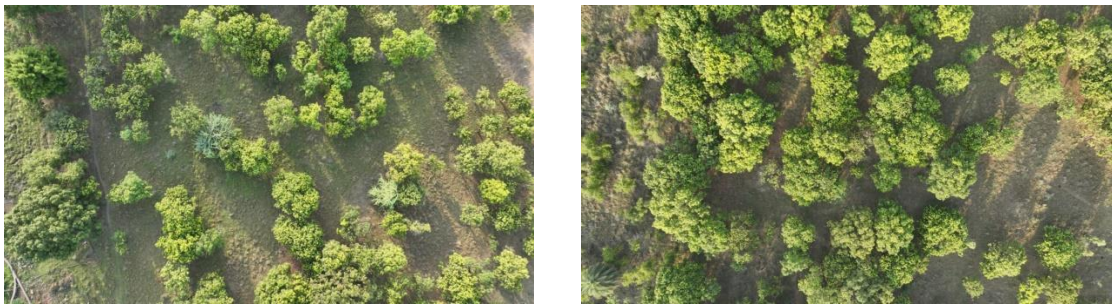

a b

Figure 3 Arial Imagery Data of treetops and shrubs for a comprehensive analysis of the area

4. Proposed Method

The work is divided into two phases. Phase one involves the use of vegetation-based indices along with CNNs and phase two focuses on prescription map generation and path planning. The model architecture is shown in Figure **4**

4.1 Weed Segmentation using Deep Learning:

We aim to use only RGB channels i.e. RGB images to predict the segmentation mask of the images. However, it becomes difficult to distinguish between crop and weed and the use of multispectral cameras is still limited to high-end applications. To resolve this we use specific vegetation indices to highlight various spectral features of the images [17]. These indices

International Journal of Applied Mathematics
Volume 38 No. 7s, 2025
ISSN: 1311-1728 (printed version); ISSN: 1314-8060 (on-line version)

namely ExG, ExGR, and CIVE can be derived using the existing RGB channel data. These help in highlighting the brightness ratios between different bands of light reflected by vegetation in images. These indices are regarded as benchmarks in vegetation segmentation [20].

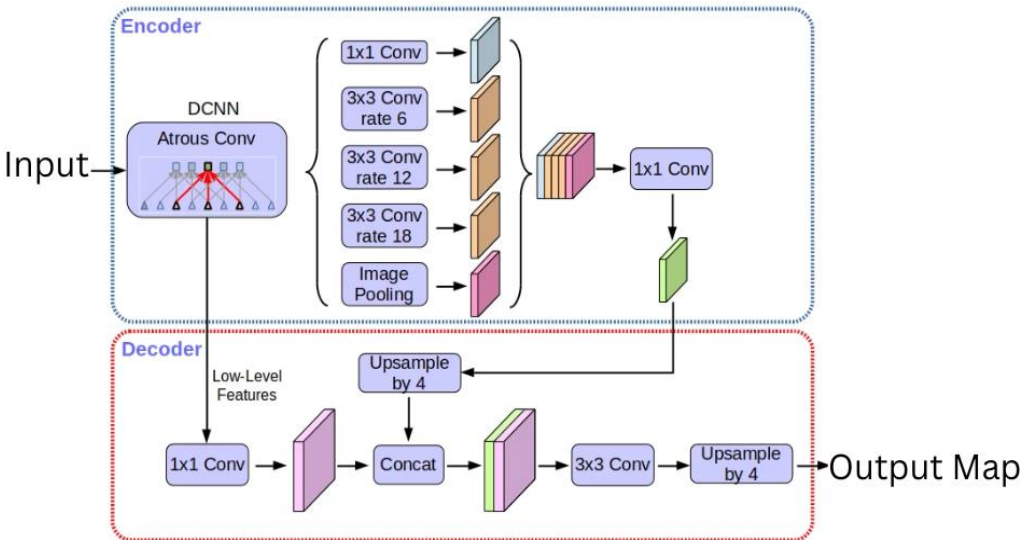

Figure 4 Model Architecture

$$ExG = 2*G - R - B \quad \textbf{(1)}$$

$$ExGR = ExG - (1.4*r - G) \quad \textbf{(2)}$$

$$CIVE = 0.441\times R - 0.811\times G + 0.385\times B + 18.78745 \quad \textbf{(3)}$$

We use the DeepLabV3+ [24] with ResNet50 as the backbone of the training model. DeepLabv3+ is a fully convolutional neural network architecture specifically designed for high-resolution semantic segmentation tasks. Its main highlight is the use of an efficient encoder-decoder structure with atrous separable convolutions. It uses a pre-trained encoder that efficiently extracts hierarchical feature maps from the input image, capturing both local and global information for semantic segmentation. Other components such as Atrous Spatial Pyramid Pooling (ASPP) can capture the multiscale information that helps differentiate between a weed and a crop. This architecture excels at semantic segmentation, where the goal is to classify each pixel in an image into a specific category. To train the deep learning model effectively, a training dataset containing high-resolution, multispectral images of agricultural fields with corresponding ground truth labels is prepared. Ground truth labels are essentially pixel-wise annotations that identify weeds and other relevant features like healthy crops and bare soil. Intersection over Union (IoU) is used to quantify the model's segmentation accuracy.

Received: August 09, 2025

Volume 38 No. 7s, 2025
ISSN: 1311-1728 (printed version); ISSN: 1314-8060 (on-line version)

4.2 Weed Infestation Assessment and Prescription Map Generation:

The final phase involves weed infestation assessment and calculation of prescription maps for variable rate application (VRA). The trained deep-learning model from the previous phase is used to predict a segmentation mask for a new image captured from the field. This mask assigns a class label (weed or non-weed) to each pixel in the image. By analyzing the segmentation mask, the total area occupied by weeds within the field can be calculated, providing a quantitative measure of weed infestation severity.

We utilized drone imagery to map fields and stitch images together to form a map of the whole field. To determine the real-world coordinates of pixels within these images, we employed a georeferencing process.

To efficiently process the entire field, we divided the map into grid patches, ensuring they were compatible with our segmentation network. After processing each patch and stitching them together, we generated a comprehensive weed mask for the entire field. To refine the segmentation output, we employed Gaussian filtering and morphological transforms to eliminate noise and smaller patches, enhancing the spatial clarity of the weed mask. Additionally, considering the UAV's spray radius, we further subdivided the field into patches to optimize weedicide application. The density of weed patches is calculated using the following equation.

$$D = \frac{W}{T} \qquad \textbf{(4)}$$

Where D is Average weed density in a patch

W is Number of weed pixels in a patch

T is Total pixels

Weed percentage within each patch is then utilized along with other factors to calculate the required amount of weedicide, facilitating the creation of a precise prescription map for drone spraying operations.

4.3 Spray Path Optimization

Once the prescription maps are obtained the data can be used to analyse the general distribution of quantity in question. This later can be used to generate a path for drone spraying operations. We implemented 3 different complete coverage path planning of the task algorithms. Once prescription maps are acquired, they serve as the foundation for analyzing the overall distribution of the relevant quantity. This data analysis forms the basis for generating optimal paths for drone spraying operations. In this study, we developed and implemented three distinct algorithms for complete coverage path planning of the task. Each algorithm was designed to efficiently navigate the terrain and ensure thorough application of the prescribed quantities. Below, we provide detailed explanations of the methodologies employed in these algorithms to achieve comprehensive coverage and effective distribution:

Received: August 09, 2025

International Journal of Applied Mathematics
Volume 38 No. 7s, 2025
ISSN: 1311-1728 (printed version); ISSN: 1314-8060 (on-line version)

a. **Lawnmower path planning**: A lawnmower path systematically covers a designated area by mimicking the pattern of mowing in rows. The algorithm, illustrated in **Figure 5**, uses field boundary coordinates (xi,yi)(x_i, y_i)(xi,yi) and initializes from a starting point (x0,y0) (x_0, y_0)(x0,y0) with a defined direction (θ). It ensures complete area coverage by generating a path that avoids overlapping and accounts for obstacles. Upon encountering a boundary or obstacle, the algorithm executes a 90-degree turn and resumes coverage until the area is fully traversed. Optimizations like dynamic direction adjustments or prioritizing specific zones can enhance efficiency based on the field's shape and conditions.

Algorithm 1 Lawnmower Path Planning

Require: Area Boundaries
Ensure: the Path covering the entire area
1: $area, (sp, dir), path, cp \leftarrow$ DefineArea(), Initialize(), [], sp
2: **while** areaNotCovered($area$, $path$) **do**
3: $bp \leftarrow$ moveUntilBoundary(cp, dir, $area$, $path$)
4: $dir \leftarrow$ turn(dir)
5: $cp \leftarrow$ continueMoving(bp, dir) ; $path.append(cp)$
6: **end whilereturn** $path$

a b

Figure 5 (a) Example of Lawnmower path, (b) Algorithm for Path planning

b. **The Priority-Based Path Planning**: This algorithm adopts a dynamic and adaptable approach to path planning by prioritizing nodes based on their prescription values, as shown in **Figure 6**. Higher-value nodes P_{ij} are addressed first, while a threshold $P_{Threshold}$ excludes low-priority nodes to prevent inefficient paths. Key metrics like power savings, coverage completeness, and adaptability guide its performance. The algorithm initializes by defining field characteristics and parameters, calculates node priorities, and optimizes paths for efficient execution of Hot-Point Missions [12], ensuring precise and prioritized spraying.

Algorithm 2 Proirity-Based Spraying Algorithm

Require: Field with weed patches, Start point, Weed threshold
Ensure: Optimal path covering all patches
1: $unsprayed \leftarrow$ GetUnsprayedPatches(field, threshold)
2: $path \leftarrow$ [start]
3: **while** unsprayed not empty **do**
4: $current \leftarrow$ last($sprayed$)
5: $scores \leftarrow$ WeedicideScores($field$, $current$, $unsprayed$)
6: $distance \leftarrow$ DistanceScores($current$, $unsprayed$)
7: $combined \leftarrow$ CombineScores($scores$, $distance$)
8: $next \leftarrow$ SelectPatch($unsprayed$, $combined$)
9: $path$.append($next$)
10: $unsprayed$.remove($next$)
11: **end whilereturn** path

Figure 6 Algorithm for Priority based spraying

c. **TSP-Based Path Planning**: This planning algorithm leverages the Traveling Salesman Problem (TSP) to optimize routes based on prescription maps, as shown in **Figure 7**. It models the field as a graph, with nodes representing points and edges denoting distances.

Received: August 09, 2025

International Journal of Applied Mathematics
Volume 38 No. 7s, 2025
ISSN: 1311-1728 (printed version); ISSN: 1314-8060 (on-line version)

Using dynamic programming, it minimizes total travel distance by solving smaller subproblems and iteratively selecting the next node with the lowest cost. The resulting optimized path ensures efficient drone operation, targeted herbicide application, reduced resource wastage, and maximum coverage, achieving the shortest route that visits all points and returns to the starting location [13].

In mathematics terms, TSP is formulated as follows:

Minimize:

$$\sum_{i \in V} \sum_{j \in V, j \neq i} x_{ij} * c_{ij} \qquad (5)$$

Subjected to:

$$\sum_{j \in V, j \neq i} x_{ij} = 1 \; for \; i \in V \qquad (6)$$

$$\sum_{j \in V, j \neq i} x_{ij} = 1 \; for \; j \in V \qquad (7)$$

$$\sum_{i \in S} \sum_{j \in S, j \neq i} x_{ij} \geq 2 \; for \; all \; non - empty \; proper \; subset \; S \subset V$$

$$x_{ij} \in \{0,1\} for \; i, j \in V$$

In this formulation:

- $\sum_{i \in V} \sum_{j \in V, j \neq i} x_{ij} * c_{ij}$ represents the total distance traveled, which we aim to minimize.
- x_{ij} is a binary decision variable that equals 1 if the tour includes the edge between nodes i and j, and 0 otherwise.
- Constraints ensure each node is visited exactly once and subtours are eliminated

Algorithm 3 Traveling Salesman Problem (Brute Force)

Require: Set of cities C and distance matrix D

```
shortestDistance ← ∞
shortestPath ← empty list
for all permutations p of C do
    currentDistance ← 0
    for all consecutive pairs of cities (i, j) in p do
        currentDistance ← currentDistance + D_ij
    end for
    if currentDistance < shortestDistance then
        shortestDistance ← currentDistance
        shortestPath ← p
    end if
end for
    return (shortestDistance, shortestPath)
```

Figure 7 TSP Algorithm

Received: August 09, 2025

International Journal of Applied Mathematics
Volume 38 No. 7s, 2025
ISSN: 1311-1728 (printed version); ISSN: 1314-8060 (on-line version)

By solving this mathematical formulation, the algorithm determines the most efficient route for the drone to follow, minimizing resource wastage and maximizing coverage. This optimized path ensures effective spraying of fertilizers and pesticides, covering all points with only a single visit by the drones.

5. Results

5.1 Segmentation Results

The dataset consists of 520 effective images i.e. is split into 80% training and 20% testing. The backbone is fed with three 448x448-channel vegetation-indexed data, which was done in the preprocessing stage shown in **Figure 8**. The images also accompany a boundary map and binary mask. The boundary map shows the region of the farmland within the image, while the binary mask displays the valid pixels within the image. We do not evaluate the regions lying outside either the boundary map or the mask. The orthomosaic images are divided into tiles which are then fed to the model. The images also accompany a boundary map and binary mask. We do not evaluate the regions lying outside either the boundary map or the mask. The model is implemented in the PyTorch framework. We trained the model using mini-batches of size 4, and uniformly rescaled the images. The training images were shuffled for each epoch. For weight initialization, we provide more emphasis on the weeds pixels as the number of background pixels is large. We use the weighted cross-entropy loss as the data is highly imbalanced. The ADAM algorithm [23] is adopted for optimization.

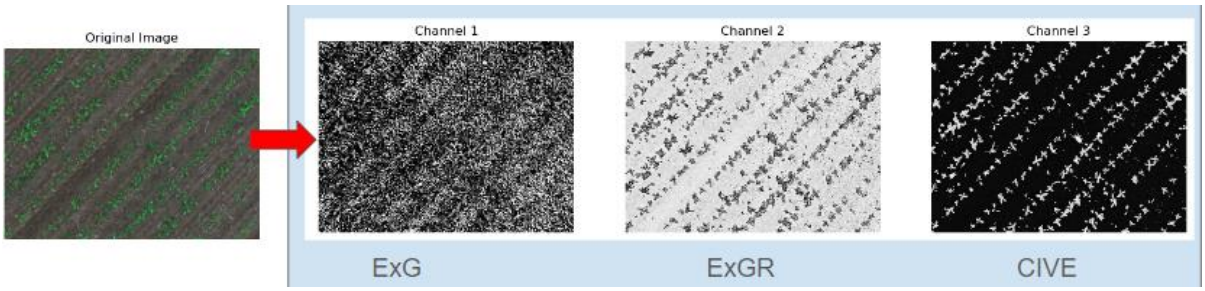

Figure 8 Pre-Processing Step using equations **(1)(2)(3)**

Table 1 Training parameters for network

Activation	**ReLU**
Learning Rate	1e-3
Batch Size	4
Epochs	20
Momentum	0.99

Received: August 09, 2025

International Journal of Applied Mathematics
Volume 38 No. 7s, 2025
ISSN: 1311-1728 (printed version); ISSN: 1314-8060 (on-line version)

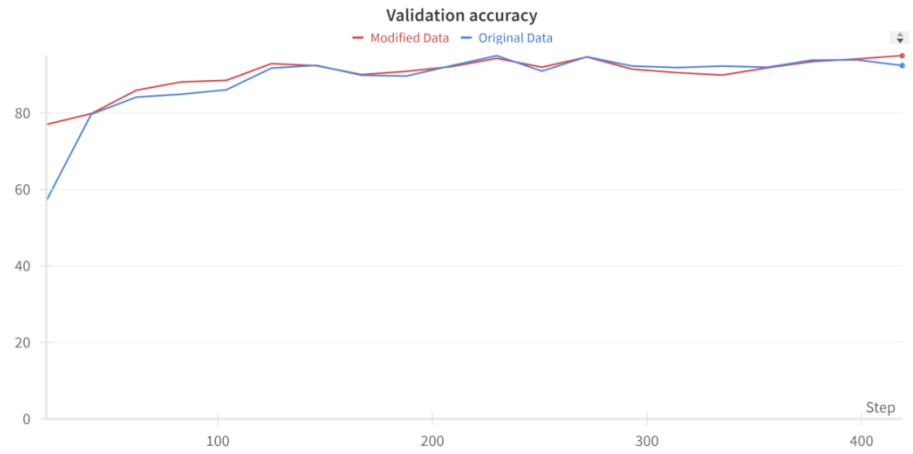

Figure 9 Validation Graph

Using the RGB-based data the model achieved an overall accuracy of 92.22% whereas with modified data it achieved 95.04%. Here accuracy mentioned is specifically to the WeedMap dataset, as it demonstrated the best performance compared to the CoFly dataset. The use of vegetation indices indicates there is a small distinction between green index of the crop and weed. The use of vegetation indices led to increase in 2.82 percent of accuracy (**Figure 9**) with a slight increase in specificity and sensitivity.

The weed circles appear to be dilated in both the cases. The use of the DeepLabv3+ along with vegetation indices did cover most of the weed patches. The results shown **Figure 10** are the comparison of both the models on the same input image.

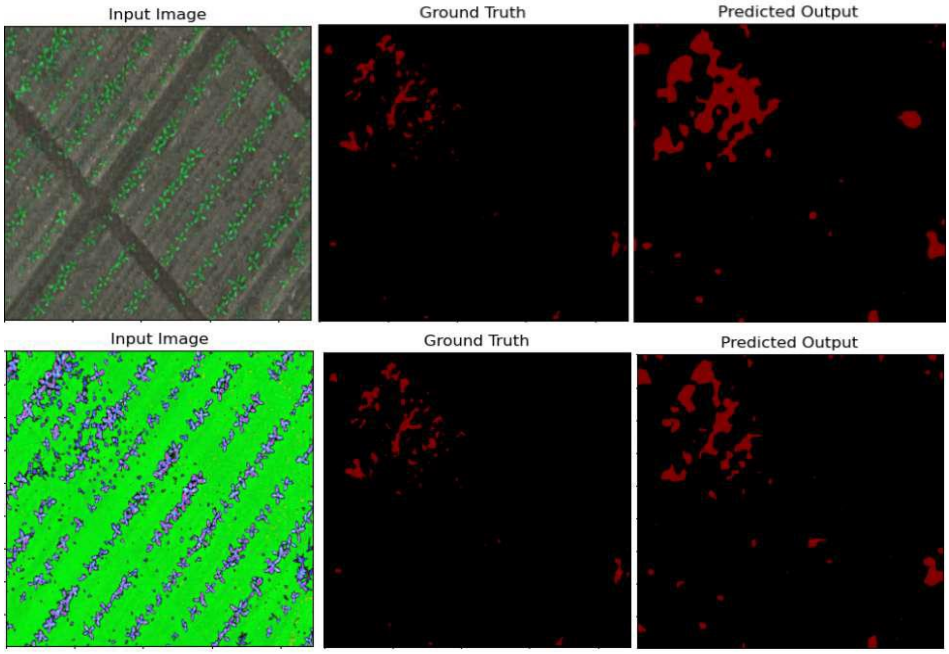

Received: August 09, 2025

International Journal of Applied Mathematics
Volume 38 No. 7s, 2025
ISSN: 1311-1728 (printed version); ISSN: 1314-8060 (on-line version)

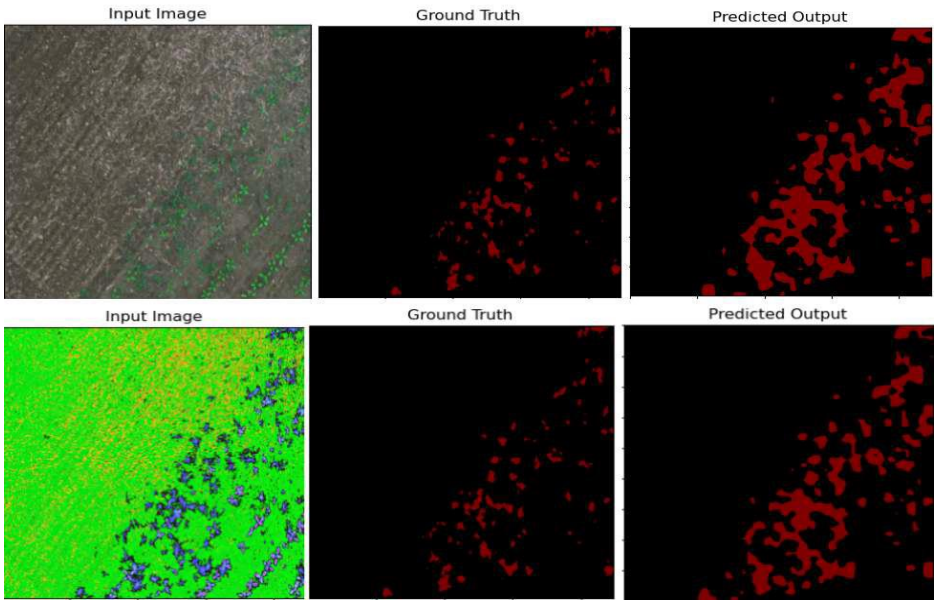

Figure 10 Quantitative result on dataset

The proposed algorithms were evaluated on the Moong dataset, representing the Indian context for plant mosaic disease detection. As shown in Figure 11, plants exhibiting yellow discoloration were classified as weeds, necessitating immediate treatment to prevent the spread of bacterial infection. During testing with real-world data, the model successfully classified the majority of infected plants. However, in certain instances, the model misclassified leguminous plants as weeds due to structural and textural similarities.

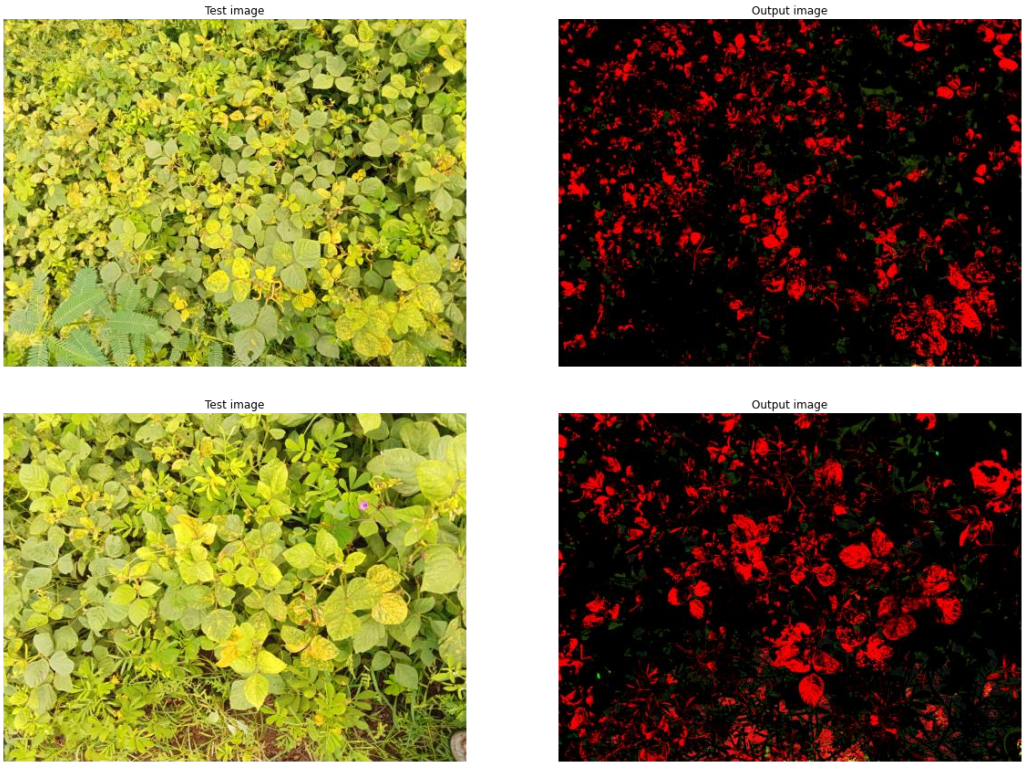

Figure 11 Images tested for Moong Dataset

Received: August 09, 2025

International Journal of Applied Mathematics
Volume 38 No. 7s, 2025
ISSN: 1311-1728 (printed version); ISSN: 1314-8060 (on-line version)

5.2 Prescription Maps and Spraying Paths

5.2.1 Prescription Maps Results

We tested our algorithm for prescription map generation on a map segment created using four images from the dataset. The images were individually processed through the weed segmentation network. The segmented masks obtained were then recombined to form the weed map of the test field, as shown in **Figure 12**. We divided the field into 4x4 patches and obtained the prescription value for each patch using a dummy formula for prescription value calculation, which takes the weed percentage in a patch as input. The visual representation of the prescription map is displayed in **Figure 13**.

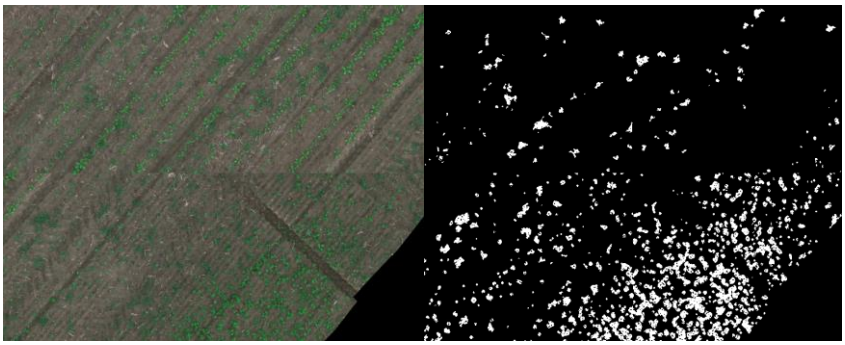

a b

Figure 12 (a) Combined Patches (b) Output Mask

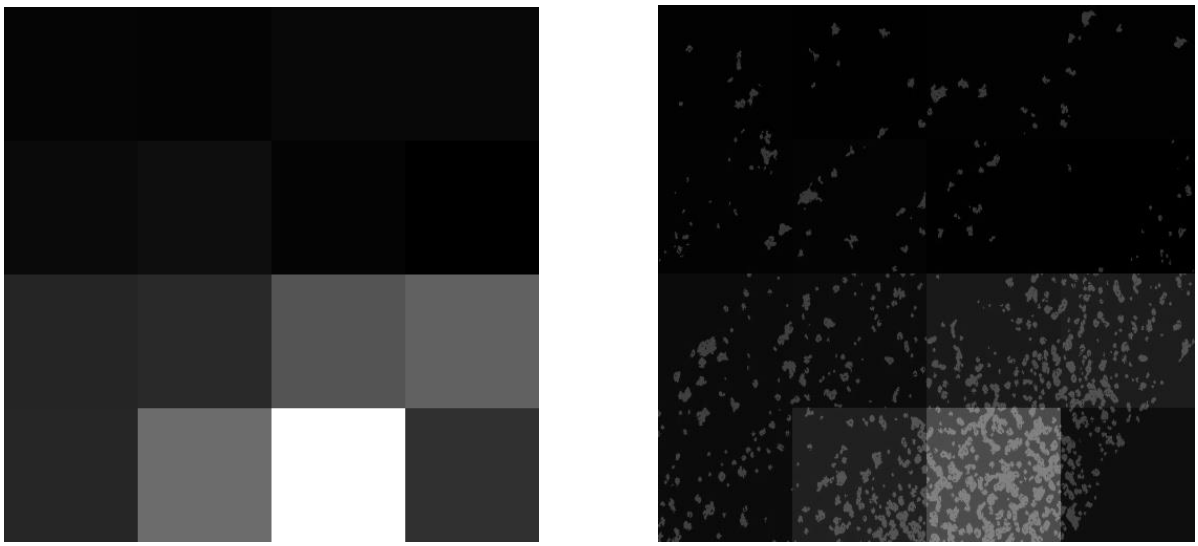

Figure 13 Prescription map

5.2.2 Comparative Study for path planning algorithms

In our study, we compared three path-planning algorithms for coverage: (1) the lawnmower algorithm (**Figure 14**), (2) the Priority-based algorithm (**Figure 15**), and (3) the TSP-based algorithm (**Figure 16**). We assessed their performance in terms of coverage, field characteristics, scalability, and suitability for given tasks prioritizing power efficiency and application effectiveness on the prescription map in **Figure 13**.

Received: August 09, 2025

International Journal of Applied Mathematics
Volume 38 No. 7s, 2025
ISSN: 1311-1728 (printed version); ISSN: 1314-8060 (on-line version)

The lawnmower path method achieves full field coverage by systematically traversing rows and columns, making it ideal for regularly shaped fields. The Priority-based algorithm prioritizes nodes based on certain criteria, such as prescription values, ensuring targeted coverage of high-value zones. We deliberately overlooked insignificant patches with lower values to prevent the generation of erratic paths. Meanwhile, the TSP-based algorithm offers an efficient path that optimally traverses cells, thereby conserving power and improving application efficiency.

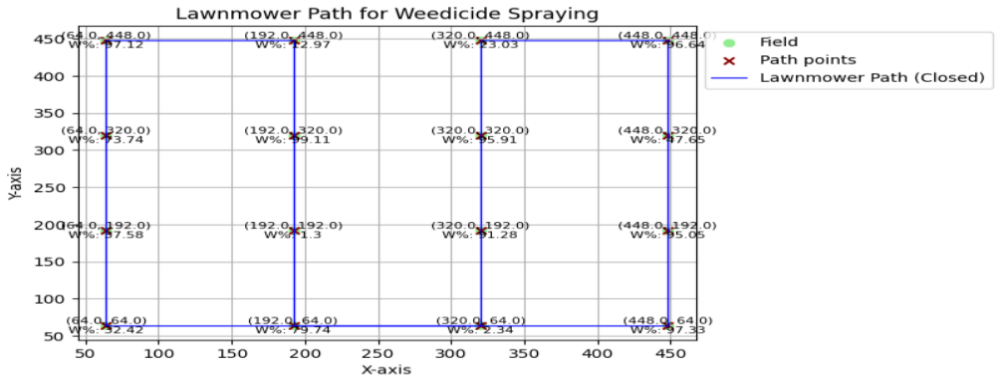

Figure 14 Lawnmower path

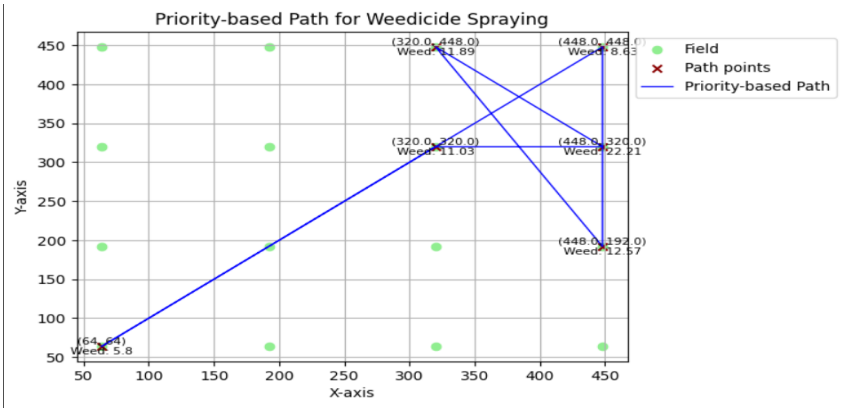

Figure 15 Priority based path

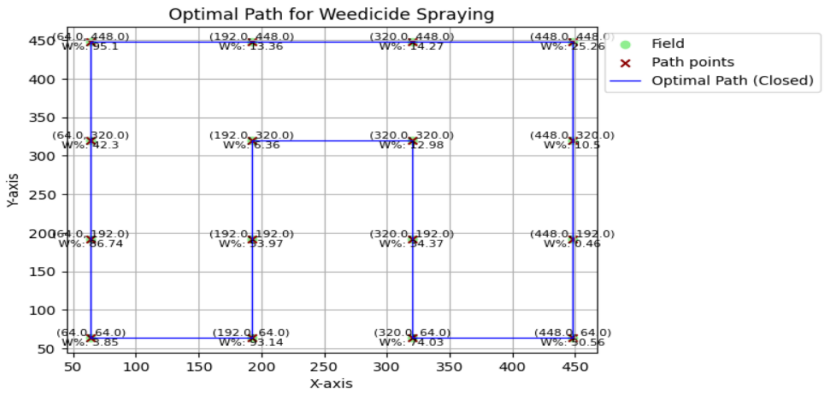

Figure 16 TSP-based approach

Received: August 09, 2025

Volume 38 No. 7s, 2025
ISSN: 1311-1728 (printed version); ISSN: 1314-8060 (on-line version)

Adaptability to field characteristics is crucial in addressing agricultural challenges. While the lawnmower path excels in efficiency for small, regularly shaped fields, its effectiveness diminishes in larger fields due to the lack of consideration for prescription values. In contrast, the Priority-Based Algorithm dynamically responds to changing conditions, concentrating resources where they are most needed. However, the computational complexity of the TSP-based algorithm may limit its efficiency in larger fields, despite its optimization capabilities, as it requires additional considerations for irregular field shapes and obstacles.

6. Conclusion

The advancement in UAV technologies can greatly help in tackling many problems faced in modern agriculture. Our work presents the use of a deep learning framework for crop weed segmentation and then generating prescription maps for the task of VRA spraying. We trained a DeepLabV3+ network using only RGB images to segment weeds from the images and utilized three spectral indices (ExG, ExGR, and CIVE) derived from the RGB channels. The model was thus trained with two different datasets: RGB and Vegetation Indices transformed images. Experimental results showed that both deep learning models led to high segmentation accuracy, but the model trained on the transformed data had an accuracy 2.82% higher than the RGB data-based model. The results indicate that the model trained on the transformed data performs better than the model trained on RGB images. This approach can help provide a cost-effective way of weed detection.

We compared different path-planning algorithms for field coverage utilizing prescription maps. Based on the three algorithms we studied, the choice of path-planning algorithm for agricultural drone applications depends on various factors, including field characteristics, task requirements, and resource constraints. While each algorithm offers distinct advantages and trade-offs, the Priority-Based Algorithm stands out for its ability to prioritize spraying in high-value areas, while the TSP-based algorithm proves more efficient when uniform coverage of crops is required, although it is computationally costly. Both of them lead to substantial power and applicant savings.

As part of our future work, we aim to develop an autonomous spraying application where prescription map data acquired from processing will be used by a sprayer drone or vehicle for precise herbicide application.

Acknowledgement

We extend our thanks to Regional Agricultural Research Station, Balasaheb Sawant Konkan Krishi Vidyapith, Raigad, Maharashtra, for allowing us to collect images of crop fields.

7. References

1. Ministry of Agriculture, India https://pib.gov.in/PressReleasePage.aspx?PRID=1741942
2. Tudi, M., Ruan, H. D., Wang, L., Lyu, J., Sadler, R., Connell, D., Chu, C., & Phung, D. T. (2021). Agriculture Development, Pesticide Application and Its Impact on the Environment. International Journal of Environmental Research and Public Health, 18(3). https://doi.org/10.3390/ijerph18031112

Received: August 09, 2025

Volume 38 No. 7s, 2025
ISSN: 1311-1728 (printed version); ISSN: 1314-8060 (on-line version)

3. Miranda-Fuentes, A., Llorens, J., Rodríguez-Lizana, A., Cuenca, A., Gil, E., Blanco-Roldán, G., & Gil-Ribes, J. (2016). Assessing the optimal liquid volume to be sprayed on isolated olive trees according to their canopy volumes. Science of The Total Environment, 568, 296-305. https://doi.org/10.1016/j.scitotenv.2016.06.013
4. Sharma, A., Kumar, V., Shahzad, B. et al. Worldwide pesticide usage and its impacts on ecosystem. SN Appl. Sci. 1, 1446 (2019). https://doi.org/10.1007/s42452-019-1485-1
5. Rajendran, S.. (2002). Pesticide Spraying in Kerala: Human Cost and Environmental Loss. Economic and Political Weekly. 37. 2206-2207. 10.2307/4412210.
6. Gil, E., Campos, J., Ortega, P., Llop, J., Gras, A., Armengol, E., Salcedo, R., & Gallart, M. (2019). DOSAVIÑA: Tool to calculate the optimal volume rate and pesticide amount in vineyard spray applications based on a modified leaf wall area method. Computers and Electronics in Agriculture, 160, 117-130. https://doi.org/10.1016/j.compag.2019.03.01
7. Satyasundar Pradhan and Subhas Chandra Jana (2023). Pesticide Tolerance Azotobacter sp., from Crop Field. Biological Forum – An International Journal, 15(6): 164-175
8. Pawase P P, Nalawade S M, Bhanage G B, Walunj A A, Kadam P B, Durgude A G, Patil M R. Variable rate fertilizer application technology for nutrient management: A review. Int J Agric & Biol Eng, 2023; 16(4): 11-19.
9. Hanif, A. S., Han, X., & Yu, S. (2022). Independent Control Spraying System for UAV-Based Precise Variable Sprayer: A Review. *Drones*, *6*(12), 383. https://doi.org/10.3390/drones6120383
10. Lou, Z., Xin, F., Han, X., Lan, Y., Duan, T., & Fu, W. (2018). Effect of Unmanned Aerial Vehicle Flight Height on Droplet Distribution, Drift and Control of Cotton Aphids and Spider Mites. *Agronomy*, *8*(9), 187. https://doi.org/10.3390/agronomy8090187
11. CHRISTENSEN, S., SØGAARD, H. T., KUDSK, P., NØRREMARK, M., LUND, I., NADIMI, E. S., & JØRGENSEN, R. (2009). Site-specific weed control technologies. Weed Research, 49(3), 233-241. https://doi.org/10.1111/j.1365-3180.2009.00696.x
12. T. Bikov, G. Mihaylov, T. Iliev and I. Stoyanov, "Drone Surveillance in the Modern Agriculture," 2022 8th International Conference on Energy Efficiency and Agricultural Engineering (EE&AE), Ruse, Bulgaria, 2022, pp. 1-4, doi: 10.1109/EEAE53789.2022.9831375.
13. Symeonaki, Eleni & Arvanitis, Kostas & Piromalis, Dimitrios & Papoutsidakis, Michail. (2020). IoT based End-to-End Farm Management System: An Approach toward Industry 4.0.
14. Ahmad, Fiaz & Khaliq, Aftab & Qiu, Baijing & Sultan, Muhammad & Ma, Jing. (2021). Advancements of Spraying Technology in Agriculture. 10.5772/intechopen.98500.
15. M. Alam, M. S. Alam, M. Roman, M. Tufail, M. U. Khan and M. T. Khan, "Real-time machine-learning based crop/weed detection and classification for variable-rate spraying in precision agriculture", Proc. 7th Int. Conf. Electr. Electron. Eng. (ICEEE), pp. 273-280, Apr. 2020.

Received: August 09, 2025

Volume 38 No. 7s, 2025
ISSN: 1311-1728 (printed version); ISSN: 1314-8060 (on-line version)

16. M. T. Chiu et al., "Agriculture-vision: A large aerial image database for agricultural pattern analysis", Proc. IEEE/CVF Conf. Comput. Vis. Pattern Recognit. (CVPR), pp. 2828-2838, Jun. 2020.
17. Xu, B., Fan, J., Chao, J., Arsenijevic, N., Werle, R., & Zhang, Z. (2023). Instance segmentation method for weed detection using UAV imagery in soybean fields. Computers and Electronics in Agriculture, 211, 107994. https://doi.org/10.1016/j.compag.2023.107994
18. Pound MP, Atkinson JA, Townsend AJ, Wilson MH, Griffiths M, Jackson AS, Bulat A, Tzimiropoulos G, Wells DM, Murchie EH, Pridmore TP, French AP. Deep machine learning provides state-of-the-art performance in image-based plant phenotyping. Gigascience. 2017 Oct 1;6(10):1-10. doi: 10.1093/gigascience/gix083. Erratum in: Gigascience. 2018 Jul 1;7(7): PMID: 29020747; PMCID: PMC5632296.
19. T. Anand, S. Sinha, M. Mandal, V. Chamola and F. R. Yu, "AgriSegNet: Deep Aerial Semantic Segmentation Framework for IoT-Assisted Precision Agriculture," in IEEE Sensors Journal, vol. 21, no. 16, pp. 17581-17590, 15 Aug.15, 2021, doi: 10.1109/JSEN.2021.3071290.
20. Sa, I.; Popović, M.; Khanna, R.; Chen, Z.; Lottes, P.; Liebisch, F.; Nieto, J.; Stachniss, C.; Walter, A.; Siegwart, R. WeedMap: A Large-Scale Semantic Weed Mapping Framework Using Aerial Multispectral Imaging and Deep Neural Network for Precision Farming. Remote Sens. 2018, 10, 1423. https://doi.org/10.3390/rs10091423
21. Xu, B., Fan, J., Chao, J., Arsenijevic, N., Werle, R., & Zhang, Z. (2023). Instance segmentation method for weed detection using UAV imagery in soybean fields. Computers and Electronics in Agriculture, 211, 107994. https://doi.org/10.1016/j.compag.2023.107994
22. Höffmann, M.; Patel, S.; Büskens, C. Optimal Coverage Path Planning for Agricultural Vehicles with Curvature Constraints. Agriculture 2023, 13, 2112. https://doi.org/10.3390/agriculture13112112
23. D. P. Kingma and J. Ba, ‘‘Adam: A method for stochastic optimization,’’
24. in Proc. Int. Conf. Learn. Representations, Jul. 2015, pp. 1–15.
25. Chen, L.-C., Zhu, Y., Papandreou, G., Schroff, F., & Adam, H. (2018). Encoder-Decoder with Atrous Separable Convolution for Semantic Image Segmentation. Proceedings of the European Conference on Computer Vision (ECCV) 2018. https://doi.org/10.1007/978-3-030-01234-2_49

Received: August 09, 2025